Role of MCP-1 on Inflammatory Processes and Metabolic Dysfunction Following High-Fat Feedings in the FVB/N Strain

Taryn L. Cranford[1], **Reilly T. Enos**[1], **Kandy T. Velázquez**[1], **Jamie L. McClellan**[1], **J. Mark Davis**[2], **Udai P. Singh**[1], **Mitzi Nagarkatti**[1], **Prakash S. Nagarkatti**[1], **Cory M. Robinson**[3], and **E. Angela Murphy**[1]

[1]Department of Pathology, Microbiology & Immunology, School of Medicine, University of South Carolina, Columbia, SC 29209, USA

[2]Department of Exercise Science, Arnold School of Public Health, University of South Carolina, Columbia, SC 29208, USA

[3]Department of Biomedical Sciences, West Virginia School of Osteopathic Medicine, Lewisburg, WV 24901, USA

Abstract

Background—MCP-1 is known to be an important chemokine for macrophage recruitment. Thus, targeting MCP-1 may prevent the perturbations associated with macrophage-induced inflammation in adipose tissue. However, inconsistencies in the available animal literature have questioned the role of this chemokine in this process. The purpose of this study was to examine the role of MCP-1 on obesity-related pathologies.

Methods—Wild-type (WT) and MCP-1 deficient mice on an FVB/N background were assigned to either low-fat-diet (LFD) or high-fat-diet (HFD) treatment for a period of 16 weeks. Body weight and body composition were measured weekly and monthly, respectively. Fasting blood glucose and insulin, and glucose tolerance were measured at 16 weeks. Macrophages, T cell markers, inflammatory mediators, and markers of fibrosis were examined in the adipose tissue at sacrifice.

Results—As expected, HFD increased adiposity (body weight, fat mass, fat percent, and adipocyte size), metabolic dysfunction (impaired glucose metabolism and insulin resistance) macrophage number (CD11b$^+$F480$^+$ cells, and gene expression of EMR1 and CD11c), T cell markers (gene expression of CD4 and CD8), inflammatory mediators (pNFκB and pJNK, and mRNA expression of MCP-1, CCL5, CXCL14, TNF-α, and IL-6), and fibrosis (expression of IL-10, IL-13, TGF-β, and MMP2) ($P<0.05$). However, contrary to our hypothesis, MCP-1

Communication: E. Angela Murphy, Department of Pathology, Microbiology & Immunology, School of Medicine, University of South Carolina, 6439 Garners Ferry Rd., Columbia SC, 29209; (803) 216-3414 (phone); (803) 216-3413 (fax); ; Email: Angela.Murphy@uscmed.sc.edu

Conflict of Interest: The authors declare no conflict of interest.

Supplementary Material
Supplementary information is available at IJO's website

deficiency exacerbated many of these responses resulting in a further increase in adiposity (body weight, fat mass, fat percent and adipocyte size), metabolic dysregulation, macrophage markers (EMR1), inflammatory cell infiltration, and fibrosis (formation of type I and III collagens, mRNA expression of IL-10 and MMP2) (P<0.05).

Conclusions—These data suggest that MCP-1 may be a necessary component of the inflammatory response required for adipose tissue protection, remodeling, and healthy expansion in the FVB/N strain in response to HFD feedings.

Introduction

Over one third of the adult population in the U.S. is obese, resulting in a rise in obesity-related conditions including heart disease, stroke, type-2 diabetes, and certain types of cancer (1-[6]). Although it is well known that obesity can be prevented through healthy dietary habits and physical activity (7, [8]), interventions in a clinical setting have generally been unsuccessful, especially in the long-term (1, [9]). Thus, changing behavior in this population has proven to be challenging. This has led to an explosion of studies to understand the pathways driving the pathologic processes associated with obesity so that therapeutic targets can be identified.

A pathophysiological mechanism that can link obesity to disease risk is chronic inflammation, a process that is largely mediated by quantitative and phenotypic changes in adipose tissue macrophages. Approximately 45-60% of adipose tissue cells express the F4/80 macrophage marker in obese mice, whereas only 10-15% of cells from lean mice express this marker (10). In addition, adipose tissue macrophages in obese mice exhibit a pro-inflammatory M1 phenotype, whereas those from lean mice have an anti-inflammatory M2 phenotype (11, [12]). Emerging evidence also associates macrophages with dysregulation of metabolic homeostasis due to their role in leptin and insulin resistance (13, [14]). Thus, targeting macrophage recruitment may reverse obesity-related pathologies.

As such, several studies have examined the role of chemokines for their ability to reduce macrophage infiltration in mouse models of diet-induced obesity. Monocyte chemoattractant protein 1 (MCP-1) is perhaps the most widely investigated chemokine in this regard. It is increased in white adipose tissue of obese subjects resulting in recruitment of bone-derived monocytes, which infiltrate the tissue from circulation (15, [16]). Recently, it has been reported that MCP-1 can even induce macrophage cell division in adipose tissue implants, whereas MCP-1 deficiency *in vivo* decreases adipose tissue macrophage proliferation (17). MCP-1 has also been implicated in playing a role in metabolism; mice engineered to express an MCP-1 transgene in adipose tissue are reported to be insulin resistant (18). However, while the majority of data supports a role for MCP-1 on high-fat-diet (HFD) related pathologies there have been some inconsistencies in the literature. For example, Inouye et al., reported no change in adipose tissue macrophage number in MCP-1 deficient mice following diet-induced obesity but in fact showed that these mice gained more weight, were glucose intolerant, had mildly increased plasma glucose and were hyperinsulinemic compared with wild-type mice suggesting a beneficial effect of this chemokine on metabolism independent of its macrophage recruiting abilities (19). While the inconsistences

in the literature are still largely unexplained, Galastri et al., reported that lack of MCP-1 differently affects inflammation according to the genetic background in a model of diet-induced steatohepatitis (20).

We sought to examine the role of MCP-1 on adiposity, cellular infiltration, inflammation, and metabolic dysfunction following HFD feeding in mice. This was done using MCP-1 deficient mice on an FVB/N background, a model that was generated in our laboratory. The HFD was designed by our research team and has previously been reported to induce obesity and increase adipose tissue macrophage infiltration following 16 weeks of feedings (21, [22]), albeit in the C57BL/6 strain.

Materials & Methods

Animals

MCP1$^{-/-}$ mice on the C57BL/6 background and FVB/N wild-type mice were originally obtained from Jackson Laboratories (Bar Harbor, ME). The FVB/N mice were crossed with the C57BL/6 MCP1$^{-/-}$ strain, and then back-crossed an additional eight times to derive the FVB/N MCP1$^{-/-}$ strain. FVB/N wild-type mice and FVB/N MCP1$^{-/-}$ mice were maintained as separate colonies but under the same conditions in the animal research facility at the University of South Carolina. Male mice were used in all experiments and were genotyped for MCP-1 using the primer sequences as follows: mutant GCCAGAGGCCACTTGTGTAG, wild type forward TGACAGTCCCCAGAGTCACA and common TCATTGGGATCATCTTGCTG. They were housed, 3-5/cage, maintained on a 12:12-h light-dark cycle in a low stress environment (22°C, 50% humidity, low noise) and given food and water *ad libitum*. Principles of laboratory animal care were followed, and the Institutional Animal Care and Usage Committee of the University of South Carolina approved all experiments.

Diets

At four weeks of age, wild-type and MCP-1$^{-/-}$ mice were randomly assigned to either a low-fat-diet (LFD) (n= 7 WT Con, n=7 MCP Con) or a HFD treatment (n=7 WT HFD, n=8 MCP HFD). Sample size was determined based on the expected effect sizes. The AIN-76A diet was used for the LFD. The HFD was designed by our laboratory and closely mimics the standard American diet (40% and 12% of calories from total fat and saturated fat, respectively) (Bioserv, Frenchtown, NJ) (21, [23]). Both diets contained similar vitamin and mineral content. Mice were fed their respective diets for 16 weeks. Two independent experiments were performed and no mice were excluded from any of the analyses.

Body weights, food intake, and body composition

Body weight and food intake were monitored weekly. Body composition was assessed approximately every 4 weeks (age 4, 9, 12, 16, and 20 weeks). Briefly, mice were placed under anesthesia (isoflurane inhalation) and were assessed for lean mass, fat mass, and body fat percentage via dual-energy x-ray absorptiometry (DEXA) (Lunar PIXImus, Madison, WI) (21).

Metabolism

Blood samples were collected from the tail vein after a 5-hour fast during week 16 of dietary treatment. Blood glucose concentrations were determined in whole blood using a glucometer (Bayer Contour, Michawaka IN). Insulin concentrations were determined in plasma using an ELISA kit (Mercodia, Uppsala, Sweden). Insulin resistance was estimated by the homeostatic model assessment (HOMA) index as follows: insulin resistance index = fasting insulin (μU/mL) $\times$ fasting glucose (mmol/L)/22.5 (24). Glucose tolerance tests were performed after 16 weeks of dietary treatment on mice fasted for 5 hours. Glucose (1g/kg) was given intraperitoneally and the blood glucose concentrations were measured intermittingly (0, 15, 30, 60, 90, and 120 minutes) over a two-hour period. Area under the curve (AUC) was calculated using the trapezoidal rule.

Tissue collection

Following 16 weeks of dietary treatment, mice were sacrificed for tissue collection. Epididymal, mesentery, and retroperitoneal fat pads as well as the liver were removed, weighed, and immediately snap-frozen in liquid nitrogen and stored at $-80°C$ or fixed in 10% formalin. All of the analyses were performed by an investigator blinded to the treatment groups.

Immunohistochemistry

A portion of epididymal adipose tissue was excised from each mouse, fixed overnight in 10% formalin, dehydrated with alcohol, and embedded in wax. Paraffin sections were stained with hematoxylin and eosin (H&E). Tissue content of type I and III collagens was examined using the picro-sirius red stain kit (Abcam, Cambridge, MA, USA, #150681).

Adipose tissue morphometry

The surface area of 100 adipocytes were determined (manual trace) from H&E stained slides using ImageJ software (National Institutes of Health, Bethesda, MD) (25) and then averaged to represent mean adipocyte size for each mouse.

Western blots

Epididymal adipose tissue was homogenized in Mueller buffer, which included a protease inhibitor cocktail (Sigma), 1% glycerophophate (100mM), 0.5% sodium orthovanadate (5mM) and 1% sodium fluoride (25mM) (21). The protein concentration was determined using the Bradford method (26). Proteins were fractioned onto Criterion precast gels (Bio-Rad, Hercules, CA) and were subsequently transferred to a polyvinylidene difluoride membrane overnight. Membranes were stained with a Ponceau S solution to verify equal protein loading and transfer efficiency. Western blot analysis was performed as previously described using primary antibodies for phosphorylated (Ser536) and total NFκB p65 (#3033S) as well as phosphorylated (Thr183/Tyr185) and total JNK (#4671S) (Cell Signaling, Danvers, MA) (27, [28]).

Magnetic cell sorting & flow cytometry

Epididymal adipose tissue samples were digested using Collagenase Type II (1mg/mL) and cRPMI (RPMI, 1% pentastrep, 1% BSA), strained, and centrifuged. Following lysing, cells were resuspended and centrifuged twice in FACS buffer to create a single cell suspension. Cells were counted and the cell volume of each sample was computed prior to pooling samples into each of the four treatment groups. An isolation buffer (PBS supplemented with 0.5% BSA and 2 mM EDTA) was used to resuspend the cells and CD11b MACS microbeads (Miltenyi Biotec Inc., San Diego, CA, #130-049-601) were used according to manufacturer's instruction. Cells were separated by magnetic properties in the column matrix (MACS, Auburn, CA, #130-042-201) and then resuspended in flow buffer. CD11b positive cells were counted using trypan blue. CD11b cells were stained for F480$^+$ (EBioscience, San Diego, CA, USA) and analyzed using a FC 500 (Beckman Coulter, Brea, CA) flow cytometer.

Real-time quantitative PCR

Epididymal adipose tissue was homogenized under liquid nitrogen using a polytron, and total RNA was extracted using TRIzol reagent (Invitrogen, Carlsbad, CA) and chloroform/ isopropyl alcohol extraction. Murine 18s rRNA was used as the housekeeping gene to normalize all of the data obtained. Quantification of epididymal adipose tissue mRNA gene expression for macrophage markers (F4/80, CD11c, CD206), T cell markers (CD4 and CD8), cytokines (interleukin-6 (IL6), tumor necrosis factor α (TNFα), interleukin-10 (IL10), and interleukin-13 (IL13)), cell proliferation and differentiation cytokine transforming growth factor β (TGFβ), chemokines (MCP-1, C-X-C motif chemokine-12 (CXCL12), C-X-C motif chemokine-14 (CXCL14), C-C motif ligand-5 (CCL5), and fetuin-A), and matrix metalloproteinases (matrix metalloproteinase-2 (MMP2), matrix metalloproteinase-9 (MMP9)), (Applied Biosystems, Foster City, CA) were performed as previously described (28). Quantitative reverse transcriptase polymerase chain reaction analysis was carried out as per the manufacturer's instructions using TaqMan Gene Expression Assays (Applied Biosystems, Foster City, CA).

Statistical analysis

All data were analyzed using commercial software (GraphPad Software, Prism 6, La Jolla, CA, USA). Total body weight, body weight percent change, body composition measurements and the glucose tolerance test were analyzed using a two-way analysis of variance at each time point. All other data were analyzed using a two-way analysis of variance. Bonferroni correction was used for all post-hoc analyses. Statistical significance was set with an α value of P ≤ 0.05 and underlying assumptions for validity of all tests were satisfied. Data are represented as mean ± SEM.

Results

FVB/N MCP1$^{-/-}$ mice fed a HFD have increased body weight gain and larger adipocyte size compared to wild-type mice fed the same diet

As expected, the HFD treatment increased body weight beginning at 1 week following initiation of the HFD treatment and remained elevated through the 16 week treatment period (Figures 1A & 1B; P<0.05). Main effects for genotype were also observed; interestingly, MCP-1 deficient mice that weighed less than WT mice at baseline (4 weeks of age) were heavier at 7-12 weeks of HFD treatment (P<0.05; Figure 1A). Percent change in body weight is presented to reflect relative changes wherein MCP-1 deficient mice experienced greater weight gain from 1-16 weeks of age (P<0.05; Figure 1B). A significant interaction was observed for body weight at weeks 9-12 and weeks 10-11 for total body weight and body weight percent change, respectively (P<0.05); MCP-1 deficient mice increased body weight only when fed a HFD.

Similar effects were seen for the body composition analysis. A main effect of diet was seen at 4, 9, 12 and 16 weeks for both body fat (Figure 1C) and body fat percent (Figure 1D) (P<0.05), and a main effect of genotype was observed at 9 and 12 weeks for both of these outcomes (P<0.05). A significant interaction was found at 9 and 12 weeks for both total body fat and body fat percent (P<0.05); the observed increase with MCP-1 deficiency was dependent on diet treatment. For lean weight, only a main effect of diet was observed at 12 weeks (Figure 1E) (P<0.05).

The HFD treatment increased mean adipocyte size regardless of genotype (Figure 1F) (P<0.05). Further, a significant interaction was found as MCP-1 deficient mice fed a HFD had a significantly larger mean adipocyte size than the wild-type HFD-fed mice (P<0.05).

Visceral fat depots (epididymal, kidney, mesenteric) and liver were collected at sacrifice and weighed (Table 1). The HFD treatment increased mass in all fat depots as well as the liver (P ≤ 0.05). Further, there was a main effect of genotype for the kidney fat weight and liver weight (P ≤ 0.05); both were heavier in MCP-1 deficient mice.

In general, there were no differences among HFD-fed mice in weekly food intake (food consumed by mice in each cage/number of mice in cage) over the course of the study.

The absence of MCP-1 in FVB/N mice fed a HFD increases insulin resistance and aggravates glucose metabolism

HFD increased fasting blood glucose (Figure 2A) and insulin concentrations, (Figure 2B) as well as the HOMA index (Figure 2C) (P ≤ 0.05). In addition, a main effect for genotype was observed where MCP-1 deficiency increased fasting blood insulin concentration and the HOMA index (P<0.05). Post-hoc analyses revealed that this effect occurred within the HFD groups only (P ≤ 0.05). A glucose tolerance test (Figure 2D, E) showed a main effect of diet (0, 15, 30, 60, 90 and 120 min) and genotype (15 and 30 min). Further, an interaction was found where MCP-1 deficient mice within the HFD treatment displayed poorer glucose metabolism than the wild-type mice at 30, 60, 90 and 120 minutes post-glucose administration (P ≤ 0.05). Consistent with the aforementioned results, the AUC also revealed

a main effect of diet and a significant interaction between the HFD treatment groups (*P* 0.05).

Adipose tissue inflammatory cell infiltration is influenced by HFD consumption and the absence of MCP-1 in the FVB/N strain

H&E staining revealed increased inflammatory cell infiltration into epididymal fat (Figure 3A). Interestingly however, MCP-1 deficiency exacerbated this response as there was a further increase in the MCP1$^{-/-}$ HFD group.

These findings were confirmed using flow cytometric analysis (Figure 3B); we report an increase in CD11b$^+$F480$^+$ cells in HFD treated mice (78.7 and 89.8% for HFD groups versus 22.6 and 27.6% for LFD groups). Again, this effect appeared to be worsened with MCP-1$^{-/-}$ within HFD as a further increase in CD11b$^+$F480$^+$ cells was observed (89.8% versus 78.7%).

RT-qPCR was performed to determine macrophage and T cell marker gene expression (Figure 3C). A significant main effect of diet was observed across all immune cell markers where HFD treatment increased EMR1 (overall macrophage), CD11c (M1 macrophage), CD206 (M2 macrophage), CD4 (T-helper cell), and CD8 (cytotoxic T cell) expression (P<0.05). A main effect of genotype was significant for EMR1 only; consistent with FACS data, MCP-1 deficiency increased expression of EMR1 and post-hoc analyses revealed that this can attributed to an elevation within the HFD treatment only (P<0.05).

Long-term HFD feeding leads to adipose tissue inflammation but this is not significantly influenced by MCP-1 in the FVB/N strain

Western blot analysis revealed a main effect of diet on pNFκB (p65) and pJNK inflammatory pathway activation (P<0.05) (Figure 4A-B). Gene expression of the chemokines MCP-1, CCL5 (Rantes) and CXCL14 were increased with HFD (P<0.05) and there was a trend for an increase in Fetuin A (P=0.09). Although there was no main effect of diet for CXCL12, there was a significant interaction where the effect of HFD was dependent on MCP-1 deficiency (P<0.05). The pro-inflammatory cytokines TNF-α and IL-6 were significantly upregulated in the HFD groups (P<0.05) (Figure 4C) but there was no effect of genotype and no interactions.

Prolonged HFD feedings leads to the formation of fibrosis in the adipose tissue of MCP-1 deficient mice on the FVB/N background

A main effect of diet was found across all 3 cytokine markers of fibrosis and tissue remodeling including IL-10, IL-13 and TGF-β (P<0.05). A main effect of genotype was observed for IL-10 (P<0.05) as well as a significant interaction between the wild-type HFD-fed mice and the MCP-1 deficient mice fed the same diet (P<0.05). There was a main effect of diet for both MMP2 and MMP9 (P<0.05); the mice treated with the HFD had significant increases in mRNA expression levels of MMP2, and conversely, decreases in mRNA expression levels of MMP9 (P<0.05) (Figure 5A). Further, for MMP2 there was a main effect of genotype and also an interaction (P<0.05); MMP2 was increased in the MCP-1 deficient mice fed a HFD compared to the wild-type group fed the same diet. Picro-sirius red

staining of the epididymal adipose tissue exhibited a substantial increase in the formation of type I and III collagens in the MCP1$^{-/-}$ HFD-fed mice (Figure 5B).

Discussion

We examined the role of MCP-1 on HFD-related pathologies using MCP-1 knockout mice on an FVB/N background. As expected, we found an increase in fat mass, metabolic dysfunction, immune cell infiltration, and inflammatory processes with HFD feedings. However, contrary to what we hypothesized, our findings indicate that MCP-1 deficiency leads to an increase in many of these HFD-related pathologies, implicating a potential necessary role for this chemokine in adipose tissue protection, remodeling, and healthy expansion.

We have previously reported that HFD feedings leads to increased adiposity, macrophage accumulation, and inflammation following 16 weeks of treatment in the C57BL/6 mouse strain (21, [27]). In the current investigation, we used mice on the FVB/N background; a strain that is often implicated as being resistant to diet-induced obesity (29-[31]). However, not all of the literature has pointed towards resistance to diet-induced obesity in the FVB/N strain as increases in body weight, plasma insulin levels, and fat pad weights in FVB/N mice fed a HFD have been documented (32). The reported inconsistences may be due to the duration of HFD feedings, fat content of the diet, sex of the mice, housing conditions, and/or differences in gut microbiota. For example, we have previously reported stark differences in adiposity, macrophage accumulation, and metabolic outcomes in the C57BL/6 mouse when the content of saturated fat, but not total fat, is altered (21). Nonetheless, our findings clearly confirm an increase in HFD-related pathologies in the FVB/N strain following 16 weeks on a 40% HFD.

While the majority of the literature supports an influence of MCP-1 on inflammatory processes and metabolic disturbances in response to HFD feedings (18, [33], [34]), several studies have reported no effect of MCP-1 (35-[37]) and some have even reported that MCP-1 depletion leads to negative connotations (37). We generated an MCP-1 deficient FVB/N mouse in our lab and were interested in furthering the understanding of this chemokine in obesity-related pathologies. Largely inconsistent with the previously reported findings, we found that MCP-1 depletion increased adiposity, resulted in exaggerated metabolic dysfunction, and exacerbated infiltration of immune cells into adipose tissue following 16 weeks of HFD feedings. Adipocyte expansion and sustained inflammation are linked to fibrosis (38). Thus, we also measured fibrosis and report a substantial increase in collagens type 1 and III along with gene expression of select genes likely involved in this process including IL-10 and MMP2.

It has been reported that a reduced ability to sense and respond to pro-inflammatory stimuli at the level of the adipocyte decreases the capacity for healthy adipose tissue expansion and remodeling, which can ultimately lead to increased HFD-related pathologies, including metabolic dysfunction and fibrotic adipose tissue (39). In fact, previous research has suggested that MCP-1 may be involved in the regulation of adipogenesis. For example, it was reported that MCP-1 generated large quantities of new adipose tissue in an engineering

model designed for adipose tissue growth (40). Further, a recent study found that MCP-1 induced protein (MCP1P) induces adipogenesis in C57BL/6 mice resulting in an increase in the number of adipocytes (41). Based on this, it is plausible that a lack of MCP-1 hindered favorable adipose tissue expansion, resulting in dysfunctional adipose tissue and metabolic perturbations as exhibited by our model.

The increase in total body fat, body fat percent, and body weight in the MCP-1 deficient mice is perplexing as there was no substantial difference in food intake (data not shown) or any noticeable difference in physical activity levels between the groups. It seems unlikely that possible changes to the adipogenic process resulting from MCP-1 deficiency would result in a ~5 gram difference in body fat content between groups. Interestingly however, Inouye et al., reported a similar finding as MCP-1 deficient mice on a C57BL/6 background had increased body fat following HFD feedings (19). They speculated that the increased adiposity may have been an effect of MCP-1 absence on adipose tissue growth, as MCP-1 has been reported to induce adipocyte dedifferentiation in 3T3-L1 adipocytes by reducing triglyceride content and expression of genes expressed in mature adipocytes, such as lipoprotein lipase, adipsin, GLUT-4, aP2, β3-adrenergic receptor, and peroxisome proliferator–activated receptor-γ (42, [43]). It's unclear as to why this effect on adiposity was most prominent during the earlier time-points; it's possible that some compensatory regulatory mechanism may be preventing further weight gain in the MCP-1 deficient mice. Future studies are necessary to fully understand this process.

Given that MCP-1 is widely accepted as a chemoattractant for macrophages among other immune cells, the findings of an increase in immune cell infiltration in MCP-1 deficient mice were surprising. However, the role of MCP-1 in promoting immune cell recruitment has recently been challenged by the absence of a noticeable impact on macrophage accumulation resulting from MCP-1 genetic disruption in C57BL/6 mice (19) In fact, Kirk et al., using a similar MCP-1 knockout approach, reported higher levels of a macrophage-specific protein in multiple fat depots as well as increased adipose tissue weight in MCP-1 deficient mice on a C57BL/6 background (37). Furthermore, HFD-fed CCR2-deficient mice do not normalize macrophage content to the levels of lean animals, suggesting that macrophage recruitment is regulated by MCP-1/CCR2 independent signaling pathways (34). Thus, we examined additional chemokines in an effort to address the increased recruitment of immune cells in MCP-1 deficient mice following HFD feedings. Our data indicate a significant increase in CXCL12 in MCP-1 deficient mice fed a HFD as well as trend for an increase in fetuin A. This could explain, at least in part, the increase in immune cell infiltration in our study as others have documented a role for these chemokines in this process (44, [45]).

Emerging evidence now links T cells to obesity-mediated insulin resistance and the systemic inflammatory response. In fact, it has been reported that infiltration of CD8+ T cells precedes that of macrophages during high-fat-diet feedings and that this T cell subset is necessary for macrophage accumulation and activation during adipose tissue inflammation (46). Similarly, it has been reported that enlarged adipocytes stimulate CD4+ T cells resulting in increased inflammation (47). As many of the chemokines measured in the current investigation are not exclusive to macrophages, we also measured T cell markers to

explore the notion that T cells may be playing a compensatory role leading to the observed increase in immune cell markers and inflammatory mediators following MCP-1 deletion. As expected, we found an increase in CD4 and CD8 gene expression in the adipose tissue following high-fat-diet feedings but there was no further increase in MCP-1 deficient mice. Thus, we do not believe that T cells are driving the metabolic perturbations and increased inflammatory cell infiltration observed in the MCP-1 deficient mice in this model.

A limitation of our study is that we examined only one time-point for the majority of outcomes; our data is limited to the 16 week time-point – a time-point when there were no differences in body composition, although differences in percent change of body weight were still evident. It would have been informative to have measured the influence of MCP-1 on inflammation and fibrosis at earlier time-points when much larger differences in body composition were observed to fully evaluate the role of this chemokine in obesity progression. It is certainly possible that differences in inflammatory mediators, chemokines, and possibly other parameters, between the groups would have been detected and/or greater had we measured these outcomes at earlier time-points.

Our data clearly suggest a necessary role for this chemokine in preventing obesity-related pathologies, at least in the FVB/N strain. However, given the previous literature, which is largely confined to the C57BL/6 strain, we performed an additional study using the C57BL/6 background utilizing the exact same diet and feeding duration. Although our sample size was limited (n=4-6/group), in general, we observed either no change or a slightly beneficial effect of MCP-1 depletion on adiposity and inflammation following HFD feedings (supplementary data Figure 1). This led us to conclude that lack of MCP-1 can differentially affect metabolic and inflammatory processes according to the genetic background. In support of this hypothesis, Galastri et al., reported similar strain differences in a mouse model of steatohepatitis in which the effects of MCP-1 deficiency were markedly different between mice on a C57BL/6 background and those on a Balb/C background (20). This is not entirely surprising as mouse strains can differ in their inherent propensities to develop metabolic diseases (48-[50]). A comprehensive study by Montgomery et al., examined strain-dependent variation in obesity and glucose homeostasis in response to HFD feeding (51). Although both C57BL/6 mice and FVB/N mice gained a significant amount of body weight, exhibited deterioration in glucose tolerance, and showed evidence of macrophage infiltration into adipose tissue following 8 weeks of HFD feedings, the magnitude of the response varied across strains (51). Interestingly and of importance to the current investigation, there was an increase in gene expression of MCP-1 in the FVB/N strain but not the C57BL/6 strain (51) indicating a possible role of MCP-1 in the early events of metabolic disease in this strain.

In summary, our data suggest that MCP-1 may be a necessary component of the inflammatory response required for adipose tissue protection, remodeling, and healthy expansion in the FVB/N strain in response to HFD feedings. Although MCP-1 is clearly linked to adiposity and macrophage accumulation, the mechanistic studies that have evaluated this chemokine remain ambiguous. Future investigations incorporating multiple mouse strains, and examining several time-points of obesity development are necessary to

understand the role of this chemokine on obesity-related pathologies in order to truly evaluate the therapeutic potential of MCP-1.

Supplementary Material

Refer to Web version on PubMed Central for supplementary material.

Acknowledgements

References

1. Roberts DL, Dive C, Renehan AG. Biological mechanisms linking obesity and cancer risk: new perspectives. Annu Rev Med. 2010; 61:301–16. [PubMed: 19824817]

2. Basen-Engquist K, Chang M. Obesity and cancer risk: recent review and evidence. Curr Oncol Rep. 2011; 13(1):71–6. [PubMed: 21080117]

3. Kahn SE, Hull RL, Utzschneider KM. Mechanisms linking obesity to insulin resistance and type 2 diabetes. Nature. 2006; 444(7121):840–6. [PubMed: 17167471]

4. Ozcan U, Cao Q, Yilmaz E, Lee AH, Iwakoshi NN, Ozdelen E, et al. Endoplasmic reticulum stress links obesity, insulin action, and type 2 diabetes. Science. 2004; 306(5695):457–61. [PubMed: 15486293]

5. Olefsky JM, Glass CK. Macrophages, inflammation, and insulin resistance. Annu Rev Physiol. 2010; 72:219–46. [PubMed: 20148674]

6. Ungefroren H, Gieseler F, Fliedner S, Lehnert H. Obesity and cancer. Horm Mol Biol Clin Investig. 2015; 21(1):5–15.

7. Fox KR, Hillsdon M. Physical activity and obesity. Obes Rev. 2007; 8(Suppl 1):115–21. [PubMed: 17316313]

8. Wareham NJ, van Sluijs EM, Ekelund U. Physical activity and obesity prevention: a review of the current evidence. Proc Nutr Soc. 2005; 64(2):229–47. [PubMed: 15960868]

9. Lemmens VE, Oenema A, Klepp KI, Henriksen HB, Brug J. A systematic review of the evidence regarding efficacy of obesity prevention interventions among adults. Obes Rev. 2008; 9(5):446–55. [PubMed: 18298429]

10. Weisberg SP, McCann D, Desai M, Rosenbaum M, Leibel RL, Ferrante AW Jr. Obesity is associated with macrophage accumulation in adipose tissue. The Journal of clinical investigation. 2003; 112(12):1796–808. [PubMed: 14679176]

11. Lumeng CN, DelProposto JB, Westcott DJ, Saltiel AR. Phenotypic switching of adipose tissue macrophages with obesity is generated by spatiotemporal differences in macrophage subtypes. Diabetes. 2008; 57(12):3239–46. [PubMed: 18829989]

12. Lumeng CN, Bodzin JL, Saltiel AR. Obesity induces a phenotypic switch in adipose tissue macrophage polarization. The Journal of clinical investigation. 2007; 117(1):175–84. [PubMed: 17200717]

13. Odegaard JI, Ricardo-Gonzalez RR, Goforth MH, Morel CR, Subramanian V, Mukundan L, et al. Macrophage-specific PPARgamma controls alternative activation and improves insulin resistance. Nature. 2007; 447(7148):1116–20. [PubMed: 17515919]

14. Landgraf K, Rockstroh D, Wagner IV, Weise S, Tauscher R, Schwartze JT, et al. Evidence of early alterations in adipose tissue biology and function and its association with obesity-related inflammation and insulin resistance in children. Diabetes. 2015; 64(4):1249–61. [PubMed: 25392242]

15. Bremer AA, Devaraj S, Afify A, Jialal I. Adipose tissue dysregulation in patients with metabolic syndrome. J Clin Endocrinol Metab. 2011; 96(11):E1782–8. [PubMed: 21865369]

16. Arner E, Mejhert N, Kulyte A, Balwierz PJ, Pachkov M, Cormont M, et al. Adipose tissue microRNAs as regulators of CCL2 production in human obesity. Diabetes. 2012; 61(8):1986–93. [PubMed: 22688341]

17. Amano SU, Cohen JL, Vangala P, Tencerova M, Nicoloro SM, Yawe JC, et al. Local proliferation of macrophages contributes to obesity-associated adipose tissue inflammation. Cell Metab. 2014; 19(1):162–71. [PubMed: 24374218]

18. Kamei N, Tobe K, Suzuki R, Ohsugi M, Watanabe T, Kubota N, et al. Overexpression of monocyte chemoattractant protein-1 in adipose tissues causes macrophage recruitment and insulin resistance. J Biol Chem. 2006; 281(36):26602–14. [PubMed: 16809344]

19. Inouye KE, Shi H, Howard JK, Daly CH, Lord GM, Rollins BJ, et al. Absence of CC chemokine ligand 2 does not limit obesity-associated infiltration of macrophages into adipose tissue. Diabetes. 2007; 56(9):2242–50. [PubMed: 17473219]

20. Galastri S, Zamara E, Milani S, Novo E, Provenzano A, Delogu W, et al. Lack of CC chemokine ligand 2 differentially affects inflammation and fibrosis according to the genetic background in a murine model of steatohepatitis. Clin Sci (Lond). 2012; 123(7):459–71. [PubMed: 22545719]

21. Enos RT, Davis JM, Velazquez KT, McClellan JL, Day SD, Carnevale KA, et al. Influence of dietary saturated fat content on adiposity, macrophage behavior, inflammation, and metabolism: composition matters. Journal of lipid research. 2013; 54(1):152–63. [PubMed: 23103474]

22. Enos RT, Velazquez KT, Murphy EA. Insight into the impact of dietary saturated fat on tissue-specific cellular processes underlying obesity-related diseases. J Nutr Biochem. 2014; 25(6):600–12. [PubMed: 24742471]

23. Grotto D, Zied E. The Standard American Diet and its relationship to the health status of Americans. Nutrition in clinical practice : official publication of the American Society for Parenteral and Enteral Nutrition. 2010; 25(6):603–12. [PubMed: 21139124]

24. Matthews DR, Hosker JP, Rudenski AS, Naylor BA, Treacher DF, Turner RC. Homeostasis model assessment: insulin resistance and beta-cell function from fasting plasma glucose and insulin concentrations in man. Diabetologia. 1985; 28(7):412–9. [PubMed: 3899825]

25. Schneider CA, Rasband WS, Eliceiri KW. NIH Image to ImageJ: 25 years of image analysis. Nature methods. 2012; 9(7):671–5. [PubMed: 22930834]

26. Bradford MM. A rapid and sensitive method for the quantitation of microgram quantities of protein utilizing the principle of protein-dye binding. Analytical biochemistry. 1976; 72:248–54. [PubMed: 942051]

27. Enos RT, Velazquez KT, McClellan JL, Cranford TL, Walla MD, Murphy EA. Reducing the dietary omega-6:omega-3 utilizing alpha-linolenic acid; not a sufficient therapy for attenuating high-fat-diet-induced obesity development nor related detrimental metabolic and adipose tissue inflammatory outcomes. PLoS One. 2014; 9(4):e94897. [PubMed: 24733548]

28. Enos RT, Velazquez KT, McClellan JL, Cranford TL, Walla MD, Murphy EA. Lowering the dietary omega-6: omega-3 does not hinder nonalcoholic fatty-liver disease development in a murine model. Nutr Res. 2015; 35(5):449–59. [PubMed: 25934114]

29. Kim DH, Gutierrez-Aguilar R, Kim HJ, Woods SC, Seeley RJ. Increased adipose tissue hypoxia and capacity for angiogenesis and inflammation in young diet-sensitive C57 mice compared with diet-resistant FVB mice. International journal of obesity. 2013; 37(6):853–60. [PubMed: 22964790]

30. Le Lay S, Boucher J, Rey A, Castan-Laurell I, Krief S, Ferre P, et al. Decreased resistin expression in mice with different sensitivities to a high-fat diet. Biochemical and biophysical research communications. 2001; 289(2):564–7. [PubMed: 11716511]

31. Hu CC, Qing K, Chen Y. Diet-induced changes in stearoyl-CoA desaturase 1 expression in obesity-prone and -resistant mice. Obesity research. 2004; 12(8):1264–70. [PubMed: 15340109]

32. Anantha S, Metlakunta MS, Sahu Abhiram. Hypothalamic Phosphatidylinositol 3-Kinase Pathway of Leptin Signaling Is Impaired during the development of Diet-Induced Obesity in FVB/N mice. Endocrinology. 2008; 149(3):1121–8. [PubMed: 18048492]

33. Kanda H, Tateya S, Tamori Y, Kotani K, Hiasa K, Kitazawa R, et al. MCP-1 contributes to macrophage infiltration into adipose tissue, insulin resistance, and hepatic steatosis in obesity. The Journal of clinical investigation. 2006; 116(6):1494–505. [PubMed: 16691291]

34. Weisberg SP, Hunter D, Huber R, Lemieux J, Slaymaker S, Vaddi K, et al. CCR2 modulates inflammatory and metabolic effects of high-fat feeding. The Journal of clinical investigation. 2006; 116(1):115–24. [PubMed: 16341265]

35. Chow FY, Nikolic-Paterson DJ, Ma FY, Ozols E, Rollins BJ, Tesch GH. Monocyte chemoattractant protein-1-induced tissue inflammation is critical for the development of renal injury but not type 2 diabetes in obese db/db mice. Diabetologia. 2007; 50(2):471–80. [PubMed: 17160673]

36. Chen A, Mumick S, Zhang C, Lamb J, Dai H, Weingarth D, et al. Diet induction of monocyte chemoattractant protein-1 and its impact on obesity. Obesity research. 2005; 13(8):1311–20. [PubMed: 16129712]

37. Kirk EA, Sagawa ZK, McDonald TO, O'Brien KD, Heinecke JW. Monocyte chemoattractant protein deficiency fails to restrain macrophage infiltration into adipose tissue [corrected]. Diabetes. 2008; 57(5):1254–61. [PubMed: 18268047]

38. Zimmermann HW, Tacke F. Modification of chemokine pathways and immune cell infiltration as a novel therapeutic approach in liver inflammation and fibrosis. Inflamm Allergy Drug Targets. 2011; 10(6):509–36. [PubMed: 22150762]

39. Wernstedt Asterholm I, Tao C, Morley TS, Wang QA, Delgado-Lopez F, Wang ZV, et al. Adipocyte inflammation is essential for healthy adipose tissue expansion and remodeling. Cell Metab. 2014; 20(1):103–18. [PubMed: 24930973]

40. Hemmrich K, Thomas GP, Abberton KM, Thompson EW, Rophael JA, Penington AJ, et al. Monocyte chemoattractant protein-1 and nitric oxide promote adipogenesis in a model that mimics obesity. Obesity. 2007; 15(12):2951–7. [PubMed: 18198303]

41. Younce C, Kolattukudy P. MCP-1 induced protein promotes adipogenesis via oxidative stress, endoplasmic reticulum stress and autophagy. Cell Physiol Biochem. 2012; 30(2):307–20. [PubMed: 22739135]

42. Sartipy P, Loskutoff DJ. Monocyte chemoattractant protein 1 in obesity and insulin resistance. Proceedings of the National Academy of Sciences of the United States of America. 2003; 100(12): 7265–70. [PubMed: 12756299]

43. Gerhardt CC, Romero IA, Cancello R, Camoin L, Strosberg AD. Chemokines control fat accumulation and leptin secretion by cultured human adipocytes. Mol Cell Endocrinol. 2001; 175(1-2):81–92. [PubMed: 11325518]

44. Kim D, Kim J, Yoon JH, Ghim J, Yea K, Song P, et al. CXCL12 secreted from adipose tissue recruits macrophages and induces insulin resistance in mice. Diabetologia. 2014; 57(7):1456–65. [PubMed: 24744121]

45. Chatterjee P, Seal S, Mukherjee S, Kundu R, Mukherjee S, Ray S, et al. Adipocyte fetuin-A contributes to macrophage migration into adipose tissue and polarization of macrophages. The Journal of biological chemistry. 2013; 288(39):28324–30. [PubMed: 23943623]

46. Nishimura S, Manabe I, Nagasaki M, Eto K, Yamashita H, Ohsugi M, et al. CD8+ effector T cells contribute to macrophage recruitment and adipose tissue inflammation in obesity. Nat Med. 2009; 15(8):914–20. [PubMed: 19633658]

47. Xiao L, Yang X, Lin Y, Li S, Jiang J, Qian S, et al. Large adipocytes function as antigen presenting cells to activate CD4+ T cells via up-regulating MHCII in obesity. Int J Obes (Lond). 2015

48. Carter CP, Howles PN, Hui DY. Genetic variation in cholesterol absorption efficiency among inbred strains of mice. J Nutr. 1997; 127(7):1344–8. [PubMed: 9202089]

49. Keelan M, Hui DY, Wild G, Clandinin MT, Thomson AB. Variability of the intestinal uptake of lipids is genetically determined in mice. Lipids. 2000; 35(8):833–7. [PubMed: 10984106]

50. Fearnside JF, Dumas ME, Rothwell AR, Wilder SP, Cloarec O, Toye A, et al. Phylometabonomic patterns of adaptation to high fat diet feeding in inbred mice. PloS one. 2008; 3(2):e1668. [PubMed: 18301746]

51. Montgomery MK, Hallahan NL, Brown SH, Liu M, Mitchell TW, Cooney GJ, et al. Mouse strain-dependent variation in obesity and glucose homeostasis in response to high-fat feeding. Diabetologia. 2013; 56(5):1129–39. [PubMed: 23423668]
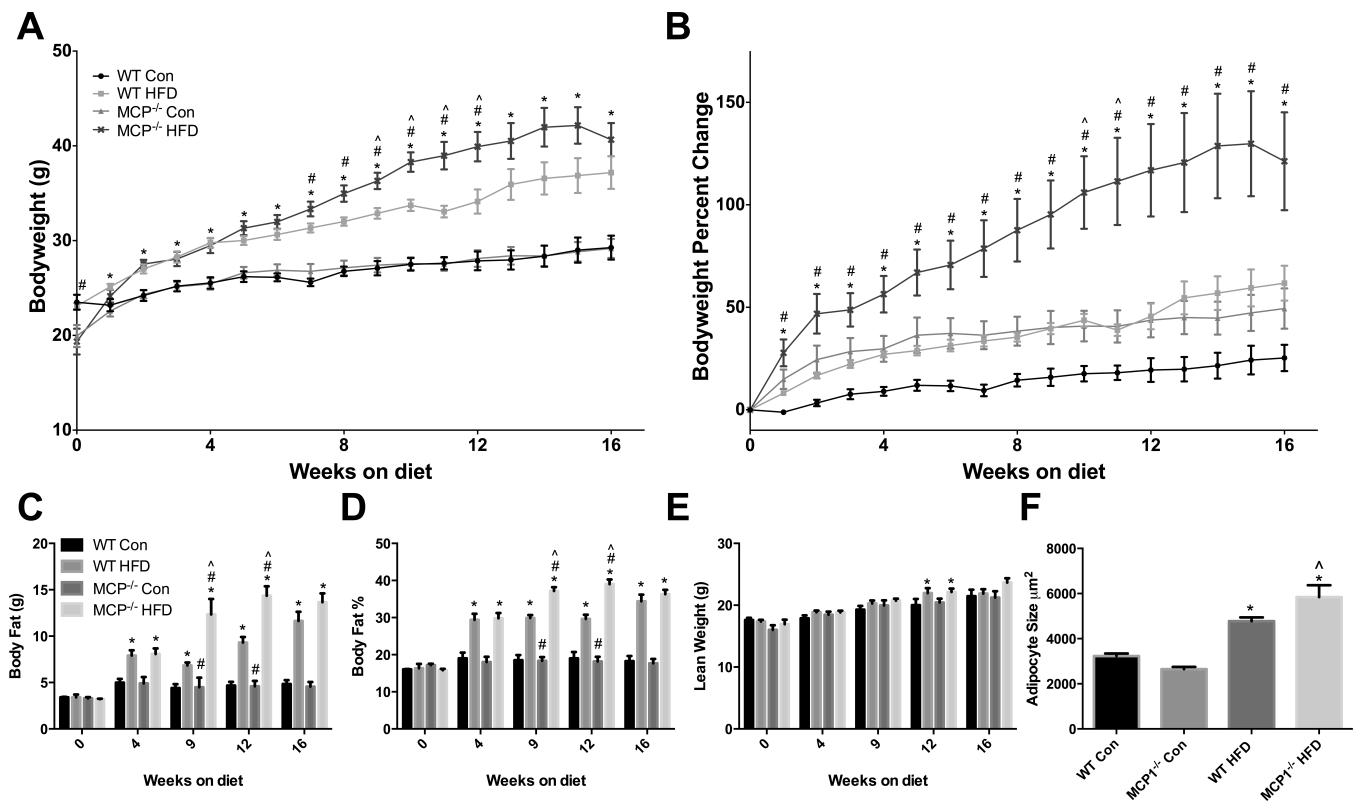
Figure 1.
Body weight characteristics. A. Body weight in grams. B. Body weight represented as percent change from starting weight. C. Body composition analysis, Body fat in grams. D. Body fat percentage. E. Lean weight in grams. F. Mean adipocyte size. *main effect of diet, #main effect of genotype. ^interaction between HFD groups. Data are represented as ± SEM and representative of two individual experiments, n=7 WT Con, n=7 WT HFD, n=7 MCP Con, n=8 MCP HFD.
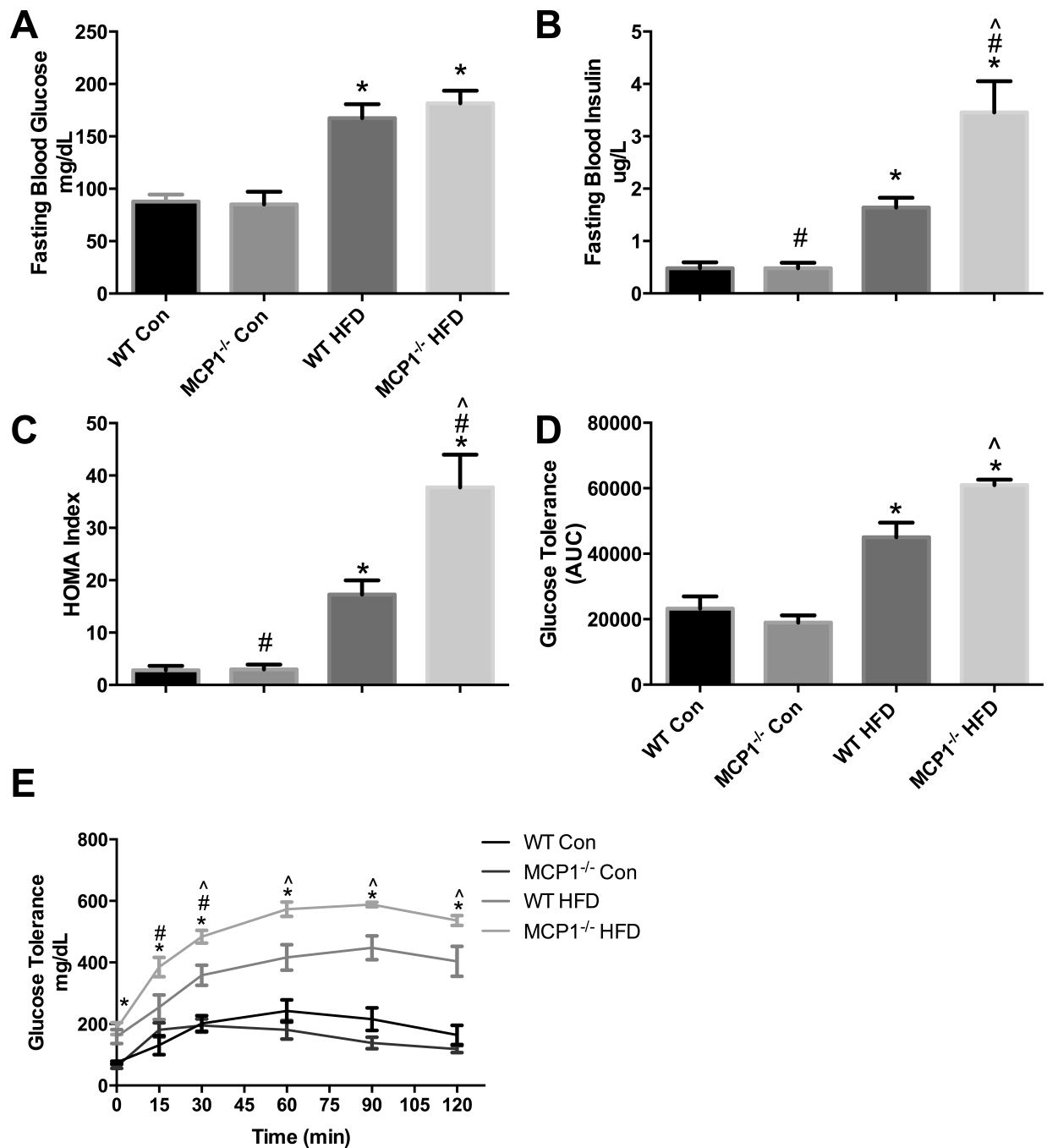
Figure 2.
Metabolic outcomes. A. Fasting blood glucose concentration (mg/dL). B. Fasting blood insulin concentration (ug/L). C. HOMA Index (n=7 WT Con, n=7 WT HFD, n=7 MCP Con, n=8 MCP HFD). D-E. Glucose tolerance test performed at 16 weeks of diet treatment (n= 4 WT Con, n=5 WT HFD, n=4 MCP Con, n=5 MCP HFD). *main effect of diet, #main effect of genotype. ^interaction between HFD groups. Data are represented as ± SEM and representative of two individual experiments.
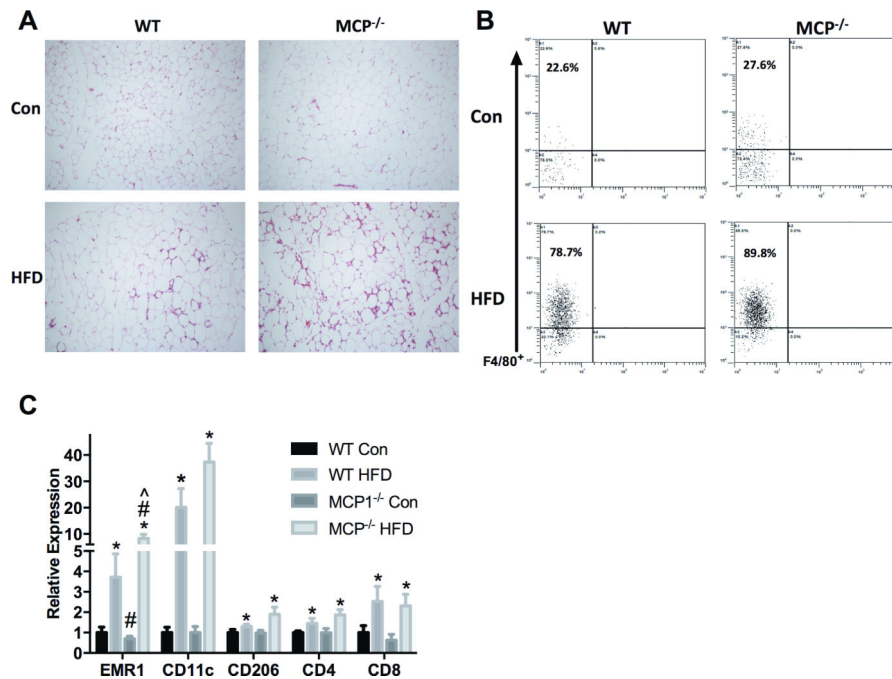
Figure 3.
Inflammatory cell population. A. Epididymal fat H&E staining. B. Flow cytometric analysis of F480$^+$ cells from cells that were positively selected for CD11b$^+$. C. Relative gene expression of macrophage and T cell markers in epididymal fat. *main effect of diet, #main effect of genotype. ^interaction between HFD groups. Data are represented as ± SEM and representative of two individual experiments, n=7 WT Con, n=7 WT HFD, n=7 MCP Con, n=8 MCP HFD.
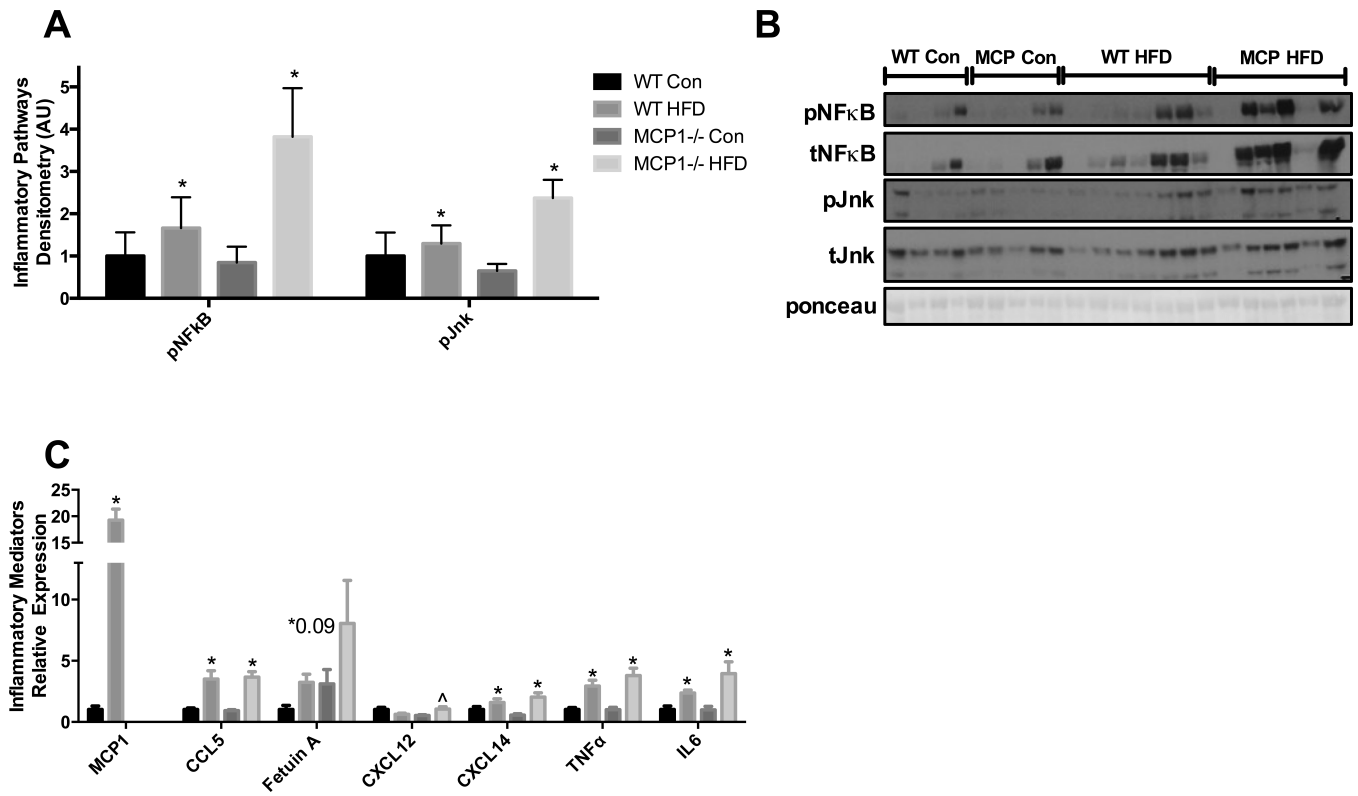
Figure 4.
Inflammatory response. A-B. Epididymal fat western blot analysis of inflammatory pathway activation. C. Relative mRNA expression of inflammatory cytokines and chemokines in epididymal fat. *main effect of diet, #main effect of genotype. ^interaction between HFD groups. Data are represented as ± SEM and representative of two individual experiments, n=7 WT Con, n=7 WT HFD, n=7 MCP Con, n=8 MCP HFD.
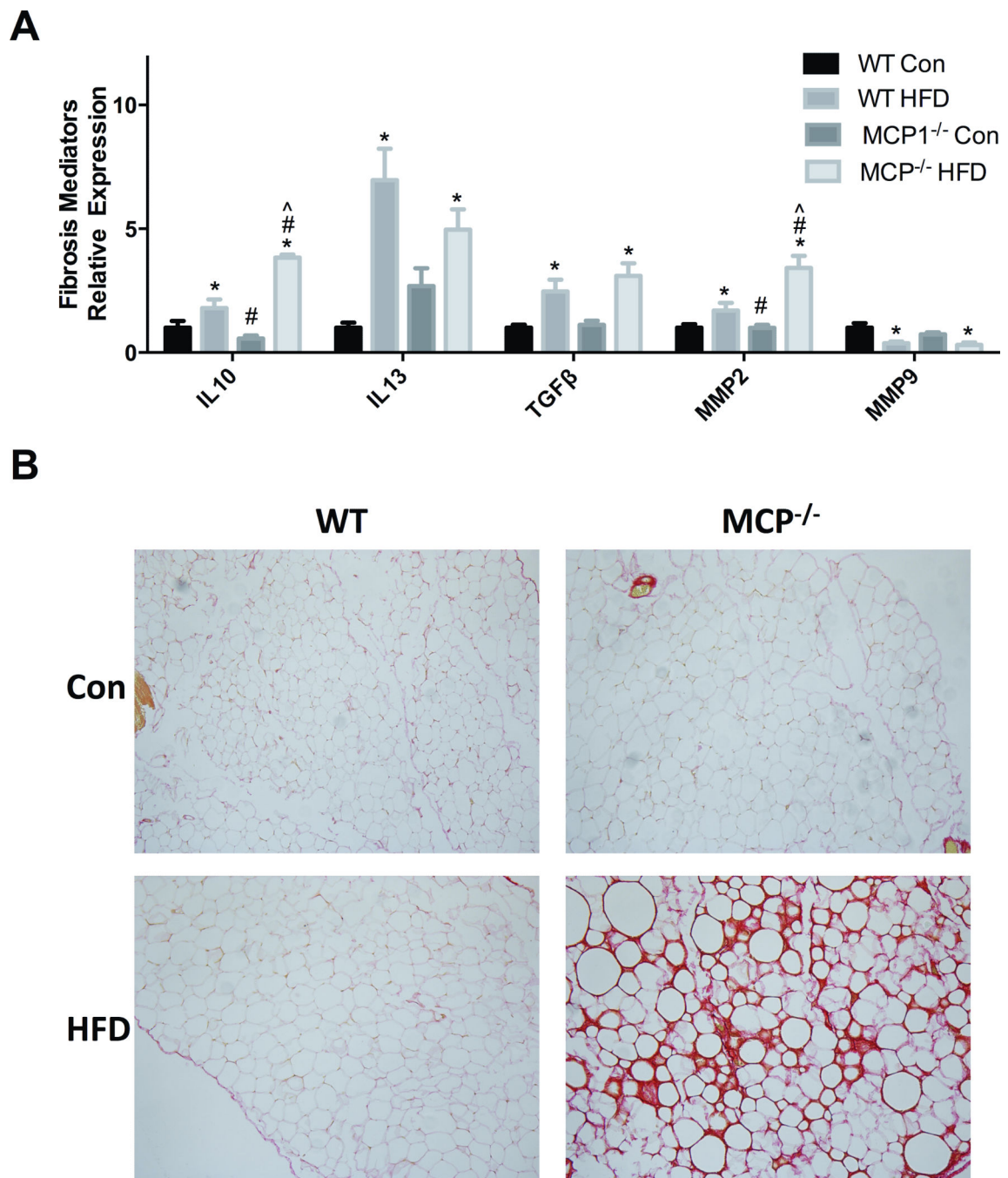
A

B

Figure 5.
Markers of fibrosis. A. Relative mRNA expression of fibrosis markers in epididymal fat. B. Picro-sirius red staining of epididymal adipose tissue. *main effect of diet, #main effect of genotype. ^interaction between HFD groups. Data are represented as ± SEM and representative of two individual experiments, n=7 WT Con, n=7 WT HFD, n=7 MCP Con, n=8 MCP HFD.

Table 1

Animal characteristics, including liver and fat pad weights, separated by mouse genotype and diet groups.

Tissue Weight (mg)	WT Control	MCP1$^{-/-}$ Control	WT HFD	MCP1$^{-/-}$ HFD
Epididymal Fat	594.4±64.5	595.1±101.5	1516.5±114.5 [*]	1313.3±117.0 [*]
Kidney Fat	302.3±42.5	389.0±78.0	978.7±56.8 [*]	1183.5±89.8 [*#]
Mesenteric Fat	430.9±39.2	431.1±56.7	1007.0±74.1 [*]	1137.4±103.1 [*]
Total Visceral Fat	1327.6±141.9	1415.3±228.0	3379.9±215.6 [*]	3634.1 ±233.6 [*]
Liver	1496.8±68.5	1667.3±73.6	1886.6±67.7 [*]	2213.0±171.8 [*#]

^interaction between HFD groups. Data are represented as ± SEM and representative of two individual experiments, n=7 WT Con, n=7 WT HFD, n=7 MCP Con, n=8 MCP HFD.

[*]
main effect of diet

[#]
main effect of genotype.